

Chapter 3

Magnetorheological Seat Suspension

The purpose of this chapter is to introduce the particular seat suspension that was used for this research. A functional configuration of the seat will be discussed, along with a functional description of the damper controller. The sensors mounted on the seat and the analog and digital circuits for processing the sensory signals and driving the MR valve are presented next.

3.1 Isringhausen Seat Suspension and Damper Controller

The seat used for this research is an Isringhausen model 7000-800, shown in Fig. 3.1. This seat is representative of the seats used in many heavy highway trucks. This particular seat suspension is known as a scissors-type suspension since the side members form an 'X' that opens and closes when the seat moves up and down. Figure 3.2 shows the scissors suspension and the locations of the critical components in the seat suspension.

An air spring that is connected to the truck air supply through a solenoid-operated valve is mounted to the crossing members A and B. The air supply valve is often connected to a leveling system that can automatically adjust the height of the seat for different driver weights. Also mounted to the crossing members is the damper. The original configuration of the seat has a standard passive damper mounted to the seat, but for this research, the passive damper has been replaced with an MR damper manufactured by Lord.

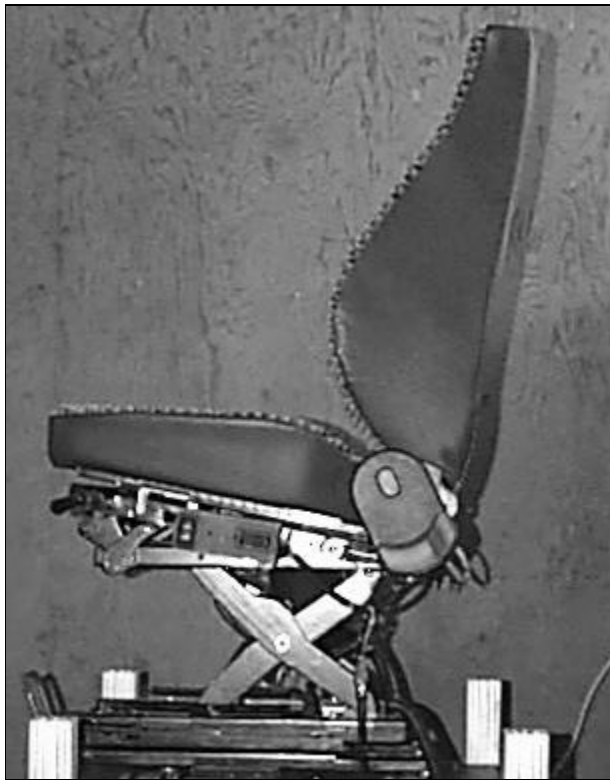


Figure 3.1. Isringhausen Seat Suspension.

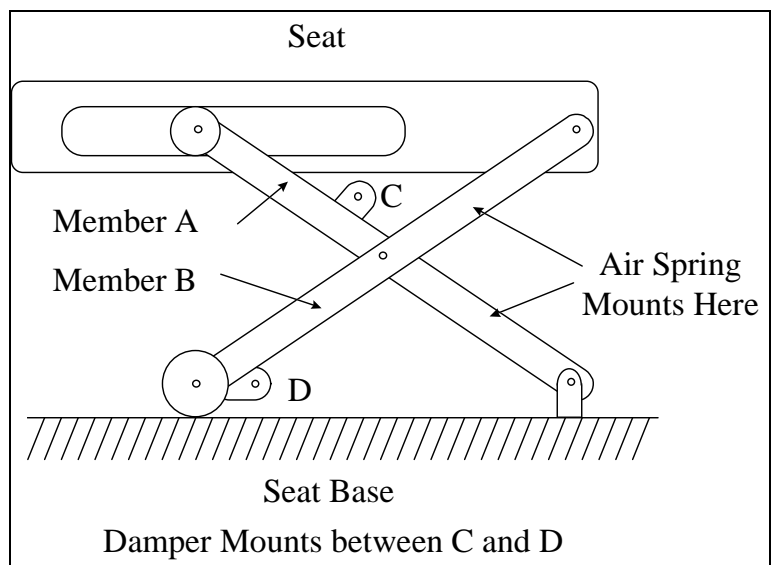


Figure 3.2. Scissors Seat Suspension.

In testing, 150 lb. of dead weight is placed on the seat to simulate the seated weight of the driver. In this configuration, the natural frequency of the seat is approximately 1.4 Hz.

The damper controller, shown in Fig. 3.3, is mounted to the seat frame analog with its associated wiring harness. The microprocessor used in the controller is a Motorola 68HC705B16 micro-controller running at an external clock speed of 4 MHz (the internal operating speed is 2 MHz). The B16 version of the 68HC05 micro-controller has eight analog-to-digital (A/D) inputs, two pulse width modulated (PWM) outputs, and a timer interrupt function. The B16 has 352 bytes of RAM, 256 bytes of EEPROM, and 15k bytes of one-time programmable (OTP) erasable-programmable, read-only memory (EPROM) that is used for control code storage. The controller was programmed to sample the sensors and act on the new information once every 1.024 ms, which corresponds to a sampling rate of about 977 Hz.

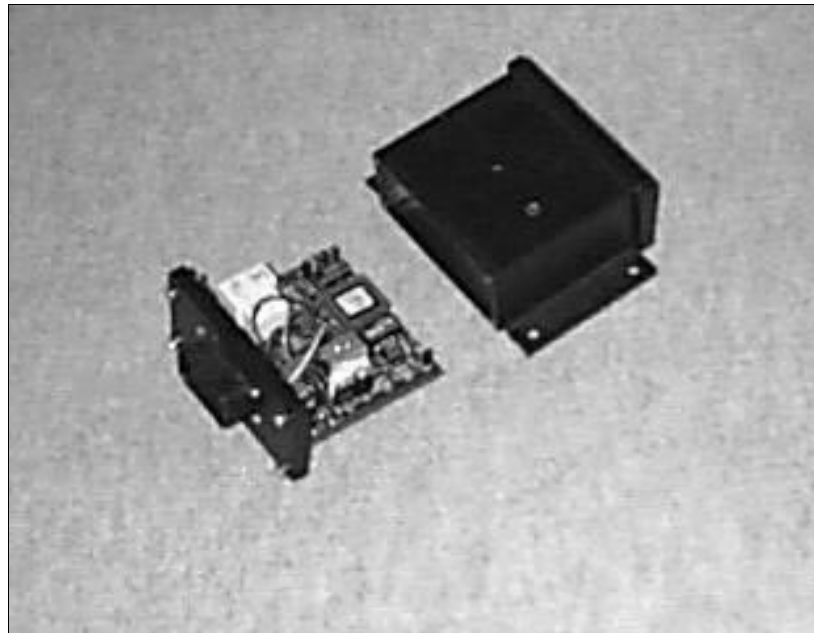


Figure 3.3. Lord Seat Controller.

3.2 Skyhook Control and the Needed Sensors

In order to identify the needed sensors, it is useful to review the requirements for skyhook control of the seat suspension. Recalling the skyhook control policy from Chapter 2,

$$\begin{cases} V_1 V_{12} > 0 & F_{SA} = C_{SKY} V_1 \\ V_1 V_{12} < 0 & F_{SA} = 0 \end{cases} \quad (3.1)$$

where:

V_1 = absolute velocity of the suspended mass with respect to the ground

V_{12} = relative velocity of the suspended mass with respect to the seat base

F_{SA} = semiactive damping force

C_{SKY} = skyhook damping coefficient

There are many ways of measuring the two velocities in Eq. (3.1). We could mount two accelerometers to the seat suspension: one could be placed on the seat base and the other could be placed on the suspended mass. By integrating the two acceleration signals, we could obtain the velocities V_1 and V_2 (Fig. 3.5). Then we could take the difference between the two signals (either in an analog fashion or digitally) to compute the relative velocity V_{12} . Since the ultimate goal of the seat suspension is to become a consumer product, a more cost-effective method is to measure V_1 using an integrated accelerometer signal and then measure the relative velocity of the seat by differentiating the position signal measured by a low-cost position sensor. The details of the position sensor are described in the following section.

3.2.1 Relative Position and the Rate Filter

The method that Lord chose to measure the velocities was to mount an accelerometer to the suspended mass and then mount a position sensor to the pivot joint in the seat suspension. The position sensor is an automotive throttle position sensor manufactured by CTS Automotive Products, which is used to measure the angle θ as shown in Fig 3.4.

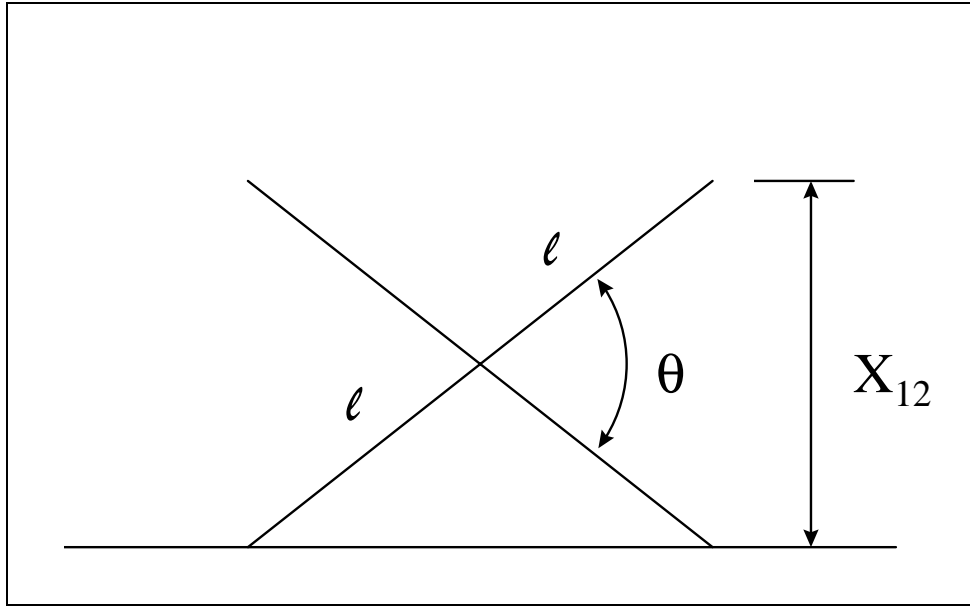


Figure 3.4. Position Measurement.

The seat height, X_{12} , can be calculated as

$$\sin \frac{\theta}{2} = \frac{\left(\frac{X_{12}}{2} \right)}{l} \quad (3.2)$$

or

$$X_{12} = 2l \sin \frac{\theta}{2} \quad (3.3)$$

where l is one-half of the 'X' member length. The suspension travel is limited by the seat height range, which is from 3 in (7.62 cm) to 9 in (22.86 cm). The half-arm length, l , is 6.5 in (16.51 cm). Therefore, we can calculate that the angle θ is limited to the range of 26° to 88° . Plotting the function $\sin \frac{\theta}{2}$ from $\theta=26^\circ$ to $\theta=88^\circ$, as shown in Fig 3.5,

indicates that $\sin \frac{\theta}{2}$ is nearly linear for this range. Thus we can approximate the functional relationship between the measured suspension angle and the seat height as a linear function, i.e.,

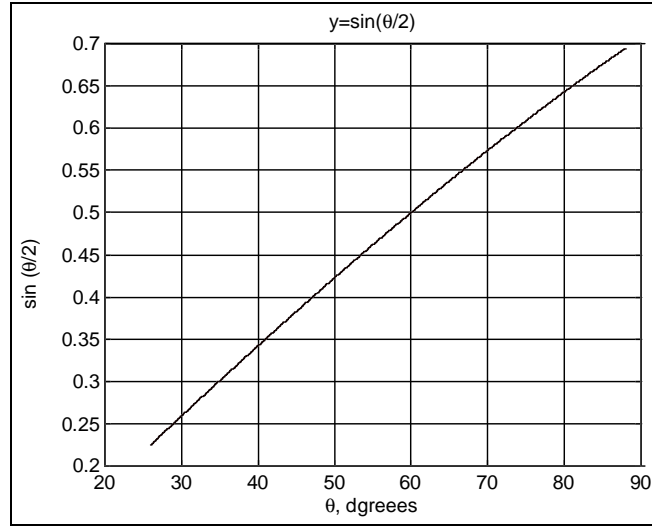


Figure 3.5. Variation of Sin($\theta/2$) Over the Measurement Range.

$$X_{12} = a\theta + b \quad (3.4)$$

where a and b are constants. Taking the derivative of X_{12} with respect to time, we obtain

$$\dot{X}_{12} = a\dot{\theta} \quad (3.5)$$

where \dot{X}_{12} is the relative velocity V_{12} . The potentiometer is a linear device and its signal can be represented as

$$\theta = cV_{POT} + d \quad (3.6)$$

where V_{POT} is the potentiometer voltage, and c and d are constants. Differentiating Eq. (3.6), we obtain

$$\dot{\theta} = c\dot{V}_{POT} \quad (3.7)$$

Substituting Eq. (3.7) into Eq. (3.6), we obtain

$$\dot{X}_{12} = ac\dot{V}_{POT} \quad (3.8)$$

Therefore, the derivative of the potentiometer voltage is directly proportional to the relative velocity across the damper. Differentiating the potentiometer signal can be quite challenging since any high frequency electrical noise will dominate the results of the differentiation.

The Lord controller processes the potentiometer voltage signal in the following manner. First, the analog signal is passed through a first-order, low-pass RC filter with a cut-off frequency of about 160 Hz. The analog signal is sampled by the controller at about 977 Hz, so this filter helps to attenuate higher frequency signals that could be aliased or cause other problems in the differentiation process.

Next, the sampled signal is passed through a digital filter, dubbed the 'Rate' filter. The Rate filter is the following sequence of instructions in the controller software:

$$\begin{aligned} \text{DISP_SUM} &= \text{DISP_SUM} - \text{DISP_AVE} + \text{DISP} \\ \text{DISP_AVE} &= \text{DISP_SUM} / \text{FILT_FREQ} \\ \text{RATE} &= \text{DISP} - \text{DISP_AVE} \end{aligned} \quad (3.9)$$

where:

DISP = latest seat displacement measurement

FILT_FREQ = constant used to change the Rate filter

RATE = output of the Rate filter

DISP_SUM and DISP_AVE are internal variables

We can develop the state-space representation for this digital algorithm and find the discrete transfer function to be

$$\frac{\text{Rate}(z)}{\text{Disp}(z)} = \frac{z[(1 - \frac{1}{F})z + (\frac{1}{F} - 1)]}{z[z + (\frac{1}{F} - 1)]} \quad (3.10)$$

where F is the variable FILT_FREQ from Eq. (3.9), which was set to 37 for this research. Plotting the discrete bode plot of the transfer function for various values of F for the controller sampling period of 1.024 ms (977 Hz sample rate) yields Fig. 3.6. At low frequencies, the phase is shifted +90 degrees, and the slope of the magnitude response is +20 dB/decade. This corresponds to a differentiation of the signal. Further, at high frequencies, the gain magnitude becomes one. This is a significant attenuation when compared to a pure differentiator, thus solving the high frequency noise problem. Although the phase shift is not exactly 90⁰ at the frequency range of interest (1-4 Hz), it is fairly close.

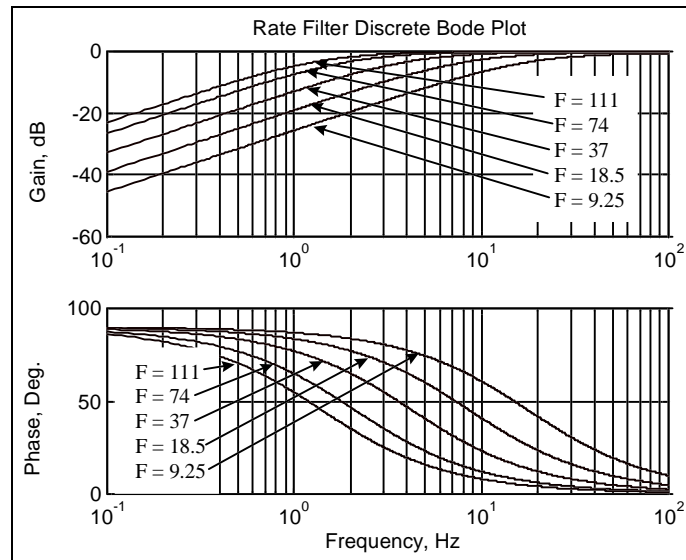


Figure 3.6. Rate Filter Variation with F.

3.2.2 Absolute Seat Acceleration and Analog Integrator

The next step is to compute the absolute velocity of the seat for the skyhook control law. This is accomplished by mounting an accelerometer to the suspended mass and using an analog integrator to compute the velocity V_1 . The accelerometer is a SCA100 Series accelerometer manufactured by VTI Hamlin. The SCA100 Series accelerometers are designed for automotive applications, so they are very compact and rugged. The SCA100 Series features internal signal conditioning so that all that is required is a 12-Volt power source. Figure 3.7 shows the accelerometer mounted to the suspension system.

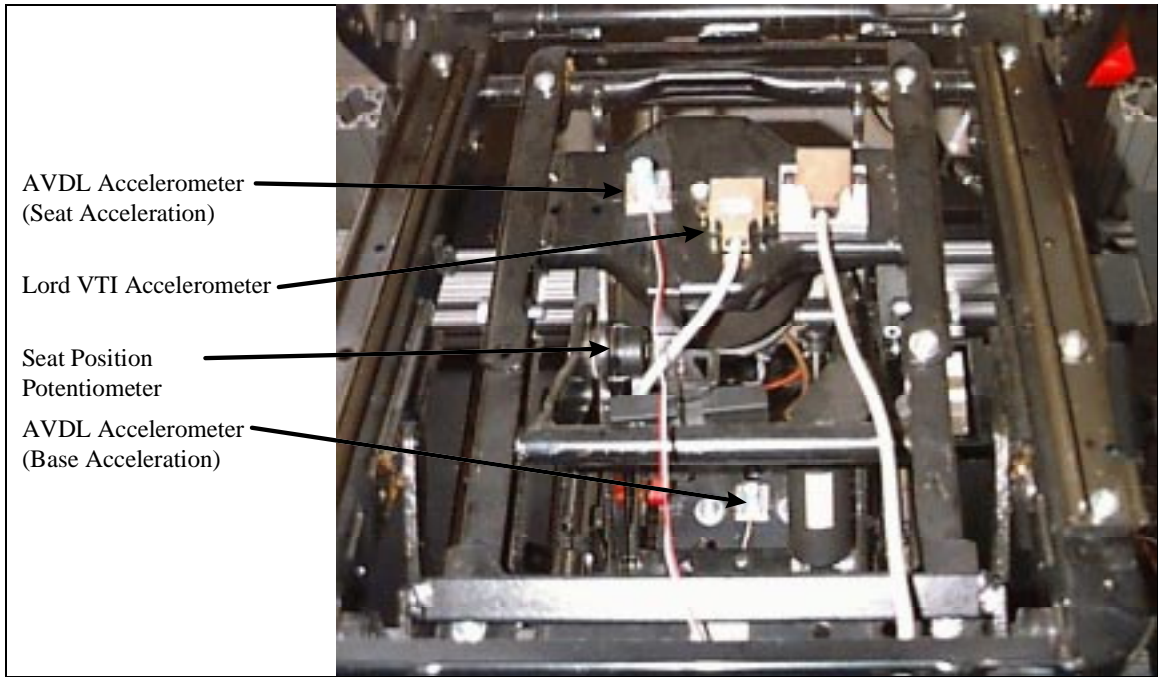


Figure 3.7. Accelerometer Position.

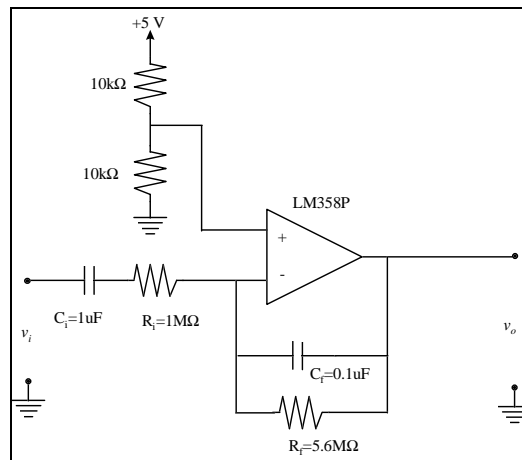


Figure 3.8. Analog Integrator Circuit.

The circuit for the analog integrator is as shown in Fig. 3.8. We can derive the transfer function of the circuit to be given by

$$\frac{v_o}{v_i} = \frac{-sC_iR_f}{C_iC_fR_iR_f s^2 + (C_iR_i + C_fR_f)s + 1} \quad (3.11)$$

The non-inverting input to the operational amplifier (op-amp) is used to add a DC offset to keep the output in the 0-5 V range in which the circuit is operating.

Using the design values of:

$$C_i = 1\mu\text{F}$$

$$C_f = 0.1\ \mu\text{F}$$

$$R_i = 1\text{M}\Omega$$

$$R_f = 5.6\text{M}\Omega$$

we can find the frequency response of the integrator as shown in Fig. 3.9. Figure 3.9 indicates that the network blocks any DC component while integrating the signals above 1.5 Hz by shifting the phase by nearly -90° and the slope of the magnitude response by $-20\ \text{dB/decade}$. At frequencies near 0.8 Hz, the phase shift is relatively close to -90° , which is acceptable for the seat controller that operates mainly in the 1-4 Hz range.

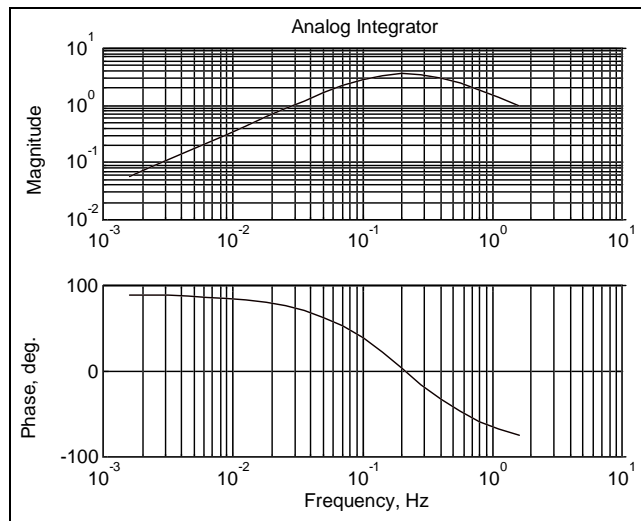


Figure 3.9. Frequency Response of the Analog Integrator.

The integrator looks like a first-order, low-pass filter, so the controller also uses it as a simple anti-aliasing filter before the signal is sampled. The sampled signal is then passed through a version of the Rate filter with $\text{FILT_FREQ} = 8192$. The discrete frequency response of this Rate filter is shown in Fig. 3.10. This filtering is performed to

remove the DC offset added by the analog integrator from the signal. The integrator inverts the velocity signal, which is accounted for in the controller software.

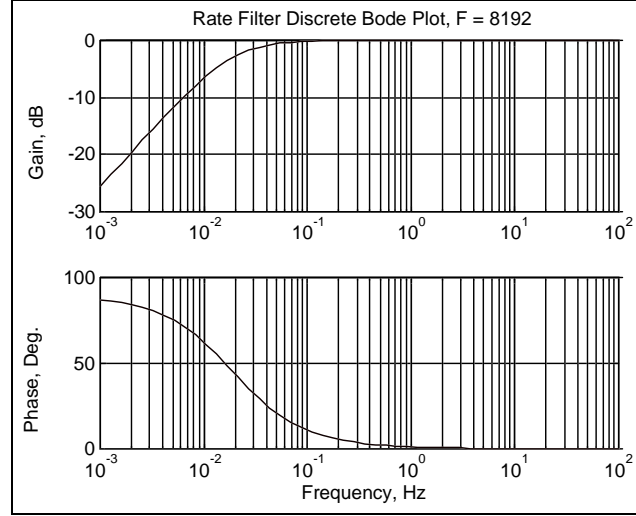


Figure 3.10. Rate Filter for Accelerometer Input.

3.3 Control Signal Reconstruction and Power Amplification

The final task to complete in order to control the MR damper is to create the control signal. From Eq. (3.1), the on-state of the damper is defined as

$$F_{SA} = C_{SKY}V_I \quad (3.12)$$

where C_{SKY} is the ideal skyhook damping coefficient. Since C_{SKY} comes from an ideal viscous damper, it is merely a constant. Combining Eqs. (3.12) and (2.7) for the damper force, we obtain

$$i = \frac{C_{SKY}}{\alpha} V_I \quad (3.13)$$

Since both C_{SKY} and α are constants, Eq. (3.13) can be reduced to

$$i = GV_I \quad (3.14)$$

where G is a user-selectable gain. In the seat controller, this gain is user-selectable since the exact value of α is unknown. The user, however, can change G until a desired seat performance criterion is met.

When the damper needs to be in the off-state, the current to the MR damper is simply turned off (i.e., $i=0$). This achieves the minimum damping that the damper can generate.

3.3.1 Control Signal Reconstruction

There are three steps that are required to reconstruct the control signal. The first two steps involve filtering the control signal. First, the pulse width modulated (PWM) signal is converted to an analog signal by passing it through a single active second-order Sallen and Key resonator filter. The Sallen and Key filter first removes the high frequency modulation from the PWM signal, leaving only the average DC value. The 68HC705 is programmed to output the PWM signal using a modulation frequency of 1953 Hz. The Sallen and Key filter is designed with a cut-off frequency of about 87 Hz.

Next, the signal is filtered through the reconstruction filter shown in Fig. 3.11. This filter is a simple, first-order, resistive-capacitive (RC) circuit designed to limit the high-frequency noise that can creep into the current drive stage of the controller.

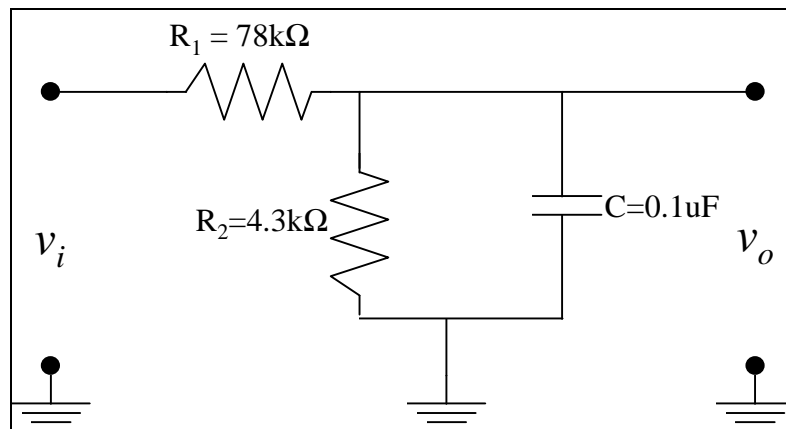


Figure 3.11. Reconstruction Filter Circuit.

3.3.2 Current Driver

The final step in creating the control signal is the current driver stage of the controller. The current driver produces a current in the MR damper, i_o , that is proportional to the

command voltage. The current driver circuit, as shown in Fig. 3.12, uses a 0.25Ω resistor, R_f , that senses the amount of current that is passing through the MR damper. The voltage dropped across the resistor is fed back to the op-amp. The op-amp then outputs a signal to the power Metal-Oxide Semiconductor Field Effect Transistor (MOSFET), which in turn adjusts the current driven through the damper. The overall gain of the current driver and first-order reconstruction filter yields an output of approximately 1 Amp for a 5-Volt input.

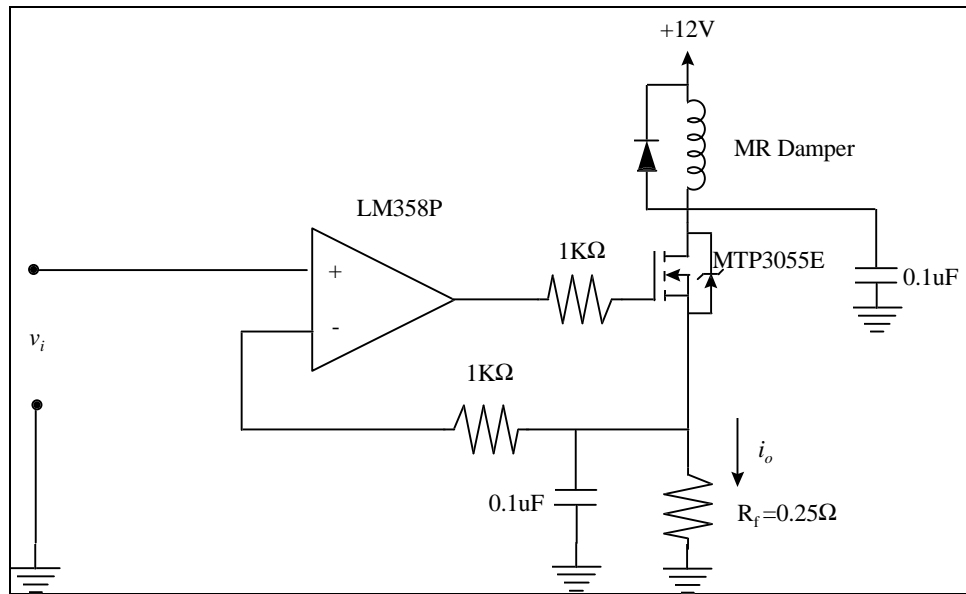


Figure 3.12. Current Driver Circuit.

3.4 Summary of Controller

Figure 3.13 summarizes the construction of the controller. The relative seat displacement signal is filtered by a first-order, low-pass filter and is then sampled by the 68HC705B16 micro-controller. The acceleration signal passes through an analog integrator and is sampled by the micro-controller. Once inside the controller, the two signals are passed through different versions of the digital Rate filter such that the velocities V_1 and V_{12} are estimated. Next, the controller uses skyhook control logic to determine the level of current that should be applied to the MR damper. This signal is

outputted as a PWM signal that is then converted to an analog signal using a Sallen and Key second-order low-pass filter. Finally, the control signal is passed through a final low-pass filter to the current driver, which develops the control current for the damper. This controller was dubbed the 'Lord Modified Rate Controller' or the Lord skyhook controller and is the main controller that was used in this research.

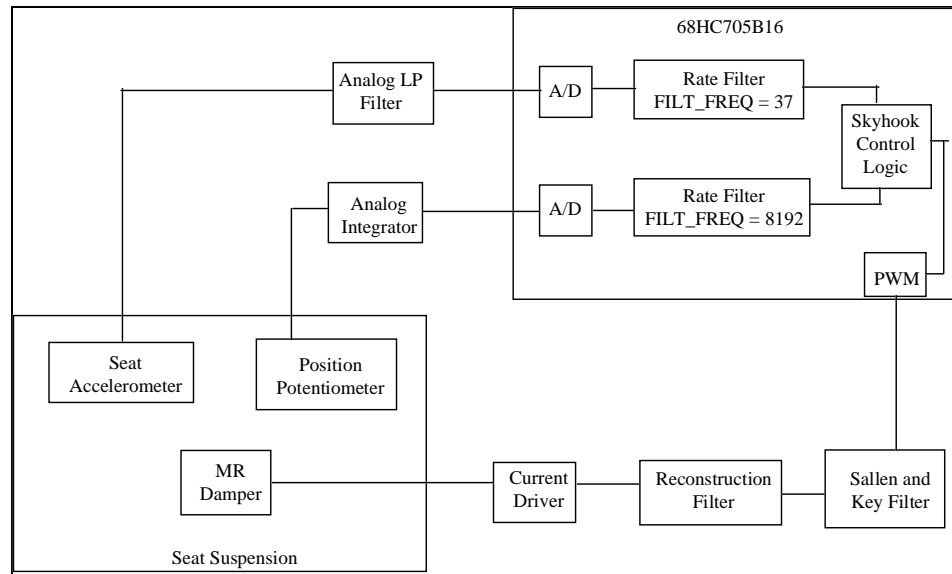


Figure 3.13. Summary of Controller Construction.